

Motion-Visual Phase-Error Detection in a Flight Simulator

Peter Grant*

University of Toronto, Toronto, Ontario M3H 5T6, Canada

and

Peter Tung Sing Lee†

Honeywell Aerospace, Mississauga, Ontario L5L 3S6, Canada

DOI: 10.2514/1.25807

An experiment was conducted on the University of Toronto Institute for Aerospace Studies Flight Research Simulator to determine the minimum phase lead of pitch motion cues relative to pitch visual cues that can be consistently detected by a human observer. The effects of pitch frequency and amplitude, motion gain, and visual scene complexity on the detection threshold of the phase error between the visual and motion cues was determined. The mean detection threshold of the phase error averaged across all subjects and conditions was 57 deg. Pitch amplitude significantly affected the detection threshold of the phase error. Higher amplitudes led to lower detection thresholds. Motion gain also had a significant effect on the detection threshold of the phase error when the frequency was 0.2 Hz or the visual complexity was low. Higher motion gains led to lower detection thresholds. The frequency had a significant effect on the detection threshold of the phase error when the motion gain was 0.5 or the visual complexity was low. Higher frequencies led to lower detection thresholds. The direction of the frequency effect suggests that subjects perform more like motion-visual phase detectors than motion-visual time delay detectors. The results of the experiment were used to analyze pitch high-pass washout filters. The analysis suggests that the break frequency for a second-order washout filter should be lower than 0.13 rad/s and the break frequency for a first-order filter should be lower than 0.2 rad/s to keep the motion-visual phase error below the measured human perception limit.

Introduction

HUMANS have multiple sensors for detecting self-motion. At very low frequencies, human motion perception is dominated by visual cues; at high frequencies, motion perception depends on a variety of sensors, including the vestibular system and somatosensory system that respond to motion through inertial space [1]. At intermediate frequencies, all of these sensors can contribute significantly to the perception of motion. In real world self-motion, all of these cues are coherent, although occasionally ambiguous. In a flight simulator, the cues are rarely coherent. In a flight simulator the computer generated visual scene is typically presented with a transport lag along with many other imperfections. The gravito-inertial cues, provided by the simulator motion system, have a phase and amplitude error that is dependent on the frequency content of the input, the dynamic response of the motion system, and the structure and tuning of the motion drive algorithm (MDA). At relatively low frequencies, the MDA generates phase lead due to the use of high-pass filters and this lead usually dominates over the phase lag of the hydraulic motion system. Therefore, at frequencies where both the visual and motion cues are important, there is usually a large phase difference between the visual and the gravito-inertial cues, with the gravito-inertial cues leading the visual cues. This phase error has the potential to reduce the controllability of the simulated vehicle, increase simulator sickness [2], and reduce the perceived fidelity of the simulation. The motion-visual phase-error effect on perceived fidelity and simulator sickness is of increased concern for modern, flexible aircraft. The addition of lightly damped, oscillatory flexible

modes to the simulator flight model will introduce sustained low-frequency aircraft motions that will in turn lead to sustained motion-visual phase errors in the flight simulator. Similarly, the motion-visual phase error is of concern for marginally stable aircraft as lightly damped oscillatory aircraft motions are also likely.

A number of previous studies [3–5] have examined the interaction between visual and vestibular motion stimuli on the perception of self-motion for both rotational and translational motion. In general, it was found that visual motion can mask inertial motion and that the addition of inertial motion to visual motion reduces the response time for perception. For yaw motion, Young et al. [3] found that visually induced motion (circular vection) can mask inertial motion in the opposite direction to the visually induced motion, and that the visual and inertial motion cues add together in a nonlinear manner to produce the perception of self-motion. Young [1] also suggests that when visual and motion cues are in conflict, the motion cues will initially dominate. Hosman and van der Vaart [4] found that the addition of inertial motion to visually induced motion reduced the response time for subjects to detect the final roll attitude resulting from the response of a second-order system to a step input in roll acceleration. Reid et al. [5] found that visually induced sinusoidal motion could mask inertial motion when it is in the same direction as the visually induced motion, particularly for frequencies below 1 Hz.

A number of studies [6,7] have also investigated the effects of delay in the visual and motion cues on pilot performance and workload. These studies found in general, that when the visual cue lags the motion cues by a significant amount (250 ms for [6] and 68 ms for [7]), pilot performance and workload are degraded. Hosman and van der Vaart [4] examined the effects of central visual, peripheral visual, and inertial motion cues on human control of a second-order vehicle model. They found that peripheral visual motion and inertial motion provided velocity information quicker (with motion being the quickest) than the central visual motion and therefore pilots could improve their control of the vehicle for disturbance and tracking tasks when either stimuli was present. Chung and Schroeder [8] examined the effects of visual-inertial motion synchronization on pilot control, handling quality ratings (HQR), motion fidelity, and perceived motion consistency for a sidestep maneuver in a helicopter simulator. The study varied the

Presented as Paper 5892 at the AIAA Modeling Simulation Technologies Conference, San Francisco, CA, 15–18 August 2005; received 12 June 2006; revision received 22 November 2006; accepted for publication 23 November 2006. Copyright © 2006 by Peter R. Grant. Published by the American Institute of Aeronautics and Astronautics, Inc., with permission. Copies of this paper may be made for personal or internal use, on condition that the copier pay the \$10.00 per-copy fee to the Copyright Clearance Center, Inc., 222 Rosewood Drive, Danvers, MA 01923; include the code 0021-8669/07 \$10.00 in correspondence with the CCC.

*Assistant Professor, Institute for Aerospace Studies, 4925 Dufferin Street. AIAA Member.

†Engineer I, 3333 Unity Drive.

delays for the visual signal, the roll motion, and the lateral motion between 45, 85, and 125 ms. The results of the study are rather difficult to interpret, but in general, a lack of synchronization between the visual and motion cues degraded pilot performance and HQR. The authors went on to suggest that the roll and lateral motion should be synchronized with each other and they should not lead the visuals, which should have a total delay of less than 100 ms. They also found that delays in the lateral motion and roll motion of the simulator could affect perceived fidelity, although somewhat surprisingly the highest fidelity did not occur at the lowest delay. In addition, although the results were difficult to generalize, they found that pilots could likely detect motion-visual synchronization errors as small as 85 ms.

To date there has been no direct measurement of the detection of the phase error between the visual and motion cues in a flight simulator. It is expected that a phase error between the visual and motion cues could lead to at least two closely related effects on the motion perception. First, there could be a reduction invection due to the conflicting motion-visual signals [1], and second the pilot may actually detect the phase error between the two signals, destroying the illusion of flight. Of particular concern in this paper is the detection of the phase error between motion and visual cues. The impact of the phase error on the perception of self-motion is also of interest to simulation engineers, but it is not directly considered in this paper. The detection of the motion-visual phase error is important for low-frequency structural vibrations, which often do not enter the pilot control loop. The phase error between the visual and motion cues in this case could have a significant effect upon the perceived fidelity of the simulation without affecting controllability. Flexible aircraft often exhibit bending modes that can lead to modest pitch and heave motion at the cockpit; see Waszak and Schmidt [9], for example. The heave motion is unlikely to lead to mismatched visual and motion cues as there is little change in the out-the-window visual scene for the modest vertical motions associated with aircraft flexing (unless in close proximity to objects). Therefore, only the detection of the phase error between the visual and motion cues for the pitching motion was examined in this study.

An experiment was conducted to determine the minimum amount of phase lead of sinusoidal pitch gravito-inertial (motion) cues relative to sinusoidal visual pitch cues that can be consistently detected by the human observer in a flight simulator environment. The study explored the effects of pitch amplitude, pitch frequency, motion gain, and visual scene complexity on the detection threshold of the phase error between the visual and motion cues. The results of the study contribute to the understanding of human motion perception and provide motion system tuners with valuable measurements.

Table 1 Experimental factors and levels

Factor	High	Low
Frequency	1.0 Hz	0.2 Hz
Amplitude (pitch velocity)	5.73 deg/s	2.29 deg/s
Motion gain	1.0	0.5
Scene complexity	High	Low

Experimental Method

The experiment was an exploratory four factor, full factorial, within subjects, repeated measures design. Two treatment levels were chosen for each factor to span a region of interest, see Table 1. An upper frequency of 1 Hz was chosen, because although flexible modes are often at higher frequencies, the visual pitch attitudes resulting from higher frequencies are extremely small for reasonable angular accelerations. A lower frequency bound of 0.2 Hz was chosen because little simulator cab motion will be generated for lower frequencies when typical high-pass washout filters are used [10]. In addition, aircraft are unlikely to have flexible modes below 0.2 Hz. The amplitudes of the sinusoidal pitch motion (pitch velocity) were determined primarily from motion base limitations and visual signal requirements. Table 2 shows the amplitudes of the corresponding visual and motion sinusoidal pitch states. As shown in Table 2, the large pitch velocity (5.73 deg/s) at 0.2 Hz leads to a pitch attitude of 4.56 deg and the large pitch velocity at 1 Hz leads to a pitch acceleration amplitude of 36 deg/s², both of which can be duplicated with unity scaling on the University of Toronto Institute for Aerospace Studies (UTIAS) motion system. The small pitch velocity (2.29 deg/s) at 1 Hz generates a maximum visual pitch attitude of only 0.37 deg, small but still above the resolution limit of the flight research simulator (FRS) visual system and the human observer [11]. The small visual pitch velocity of 2.29 deg/s is also well above the threshold of visual velocity detection [11]. The small pitch velocity (2.29 deg/s) with a motion gain of 0.5 results in a motion pitch velocity of 1.15 deg/s, which is within the human vestibular perception range [12]. A motion gain of 0.5 is typical for a flight-training device and a gain as large as 1.0 is possible for engineering simulators. The high complexity scene, shown in Fig. 1, is at an altitude of 4.6 m in front of a town with fine detail texture. The low complexity scene, shown in Fig. 2, is a sparse visual scene at an altitude of 4572 m. The two scenes were chosen to span the set of visual scene complexities used in most flight simulators.

For sinusoidal motion, only one pitch state (attitude, velocity, or acceleration) can be held constant across the two test frequencies. Pitch velocity was chosen for the amplitude factor because it fits between the visual and motion perception states. Pitch velocity is the derivative of the direct visual perception state of pitch attitude, and velocity is the integral of the direct inertial motion perception state of angular acceleration. There is also evidence that humans can estimate velocity from a visual scene [4], and the vestibular system can be considered a velocity sensor in the 0.2–1 Hz range when the vestibular system dynamics are included [13].

The detection threshold of the phase error was determined using an adaptive Levitt method [14], which is a well-established psychophysical testing procedure. This procedure was used to converge on the phase error that led to detection of the phase error 79% of the time. This phase error will be referred to (somewhat erroneously) as the phase-error detection threshold, or simply the phase-error threshold. In fact, there is no absolute threshold; there is a probability of detection that depends on the magnitude of the phase error. The probability of detection is best described by a psychometric curve [15], which is a plot of the probability of detection versus the amplitude of the signal being detected (in this case the phase lead of the motion signal relative to the visual signal). The entire curve is required to describe the complete detection

Table 2 Visual and motion sinusoid pitch amplitudes

Experimental condition			Visual pitch amplitude			Motion pitch amplitude		
Frequency, Hz	Motion gain	Amplitude, deg/s	Attitude, deg	Velocity, deg/s	Accel., deg/s ²	Attitude, deg	Velocity, deg/s	Accel., deg/s ²
0.2	1.0	5.73	4.56	5.73	7.20	4.56	5.73	7.20
0.2	0.5	5.73	4.56	5.73	7.20	2.28	2.87	3.60
0.2	1.0	2.29	1.82	2.29	2.88	1.82	2.29	2.88
0.2	0.5	2.29	1.82	2.29	2.88	0.91	1.15	1.44
1.0	1.0	5.73	0.91	5.73	36.0	0.91	5.73	36.0
1.0	0.5	5.73	0.91	5.73	36.0	0.46	2.87	18.0
1.0	1.0	2.29	0.37	2.29	14.4	0.37	2.29	14.4
1.0	0.5	2.29	0.37	2.29	14.4	0.18	1.15	7.20



Fig. 1 High complexity visual scene.

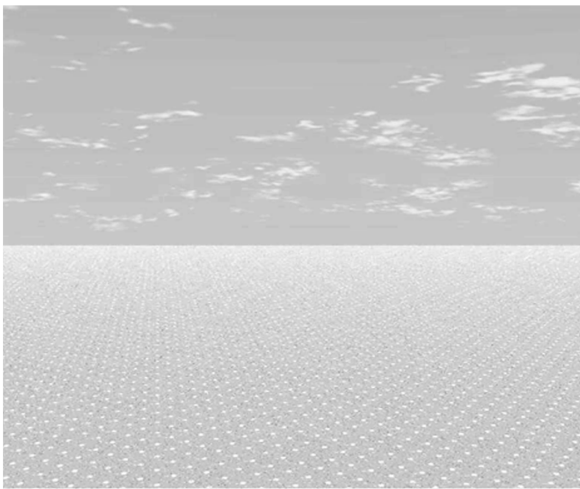


Fig. 2 Low complexity visual scene.

process. The Levitt procedure produces an accurate estimate of a single point on the psychometric curve because most of the measurements occur around the chosen probability of detection level (in this case 79%).

In this experiment, a modified 1-up 3-down response sequence was used. Each trial in the experiment consisted of two intervals, one with the motion and visuals in phase and one with the motion leading the visuals by a given amount. At the end of each trial, the subject selects the interval they believe contained the synchronized visual and motion cues. In the 1-up 3-down sequence, the phase error is reduced when three consecutive correct responses occur. One incorrect response leads to an increase in the phase error. The procedure is begun with a large phase error so the chances of an initial correct response are high. Two modifications were made to the standard Levitt 1-up 3-down procedure to increase the convergence performance. First, a 1-up 1-down sequence was used until the first reversal in the phase-error adjustment direction (decreasing to increasing or vice versa) occurred [16], at which point the 1-up 3-down procedure was used. Second, as suggested by Levitt [14], the magnitude of the phase-error adjustment was adapted during the procedure. For the first four reversals, 4 dB changes in the phase error were made. After the fourth reversal, 2 dB changes in the phase error were made. This speeds up the convergence, yet still provides precise threshold estimates toward the end of the procedure. A session was terminated after 10 reversals in phase error or 40 trials. The “threshold” is then estimated by averaging the phase error at the fifth and subsequent reversals. For cases where the run was terminated before 10 reversals and there were an odd number of trials, the threshold was estimated by averaging the phase error at the fourth

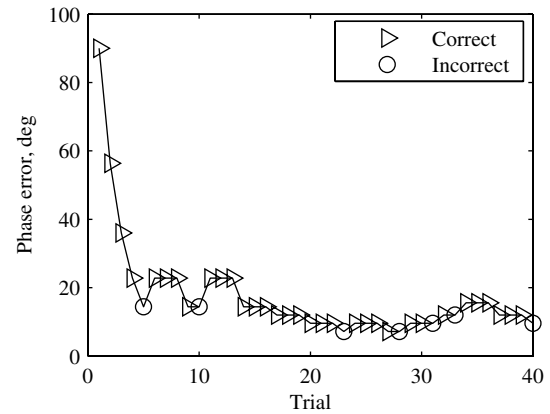


Fig. 3 Levitt procedure for subject 2.

and subsequent reversals. The total time for a session was approximately 30 min. An example of the Levitt procedure from the experiment is shown in Fig. 3. For this case, the phase-error threshold was determined to be 11.9 deg.

Experimental Setup

The experiment was conducted on the UTIAS FRS shown in Fig. 4. The FRS consists of a DC-8 simulator cab mounted on top of a CAE 300 Series hydraulic motion system. The motion system is a 0.914 m stroke, Stewart platform. The system is capable of ± 20 deg of pitch, ± 25 deg/s of pitch velocity, and ± 400 deg/s² of pitch acceleration. The system has a bandwidth (defined by the 3 dB gain point) of 10 Hz. Grant describes the motion characteristics of the system in detail [17].

A CAE Maxvue® Enhanced B image generator was used to generate the visual scene. The system, as installed at UTIAS, had a transport delay of 78 ms (from visual system command to half a screen refresh). The image was refreshed at 60 Hz noninterlaced.

A CAE fiber optic helmet-mounted display (FOHMD) system was used to display the visual images to the subject. The system has a 23 deg stereo overlap, a vertical field of view (FOV) of 37 deg, and a horizontal FOV of 71 deg. The image resolution for each eye is 1056 horizontal pixels \times 1144 vertical lines. The helmet system uses a Polhemus® magnetic head tracker to determine the position and orientation of the subject's head relative to the simulator cab. In addition, three orthogonal rate gyros mounted onto the helmet are used to generate lead for rotational head motions. The future value of the head orientation relative to the cab is estimated by multiplying the measured angular rates by 0.05 and adding these onto the orientation of the head relative to the cab. The image generator (IG) combines the sinusoidal visual pitch attitude with the future value of head

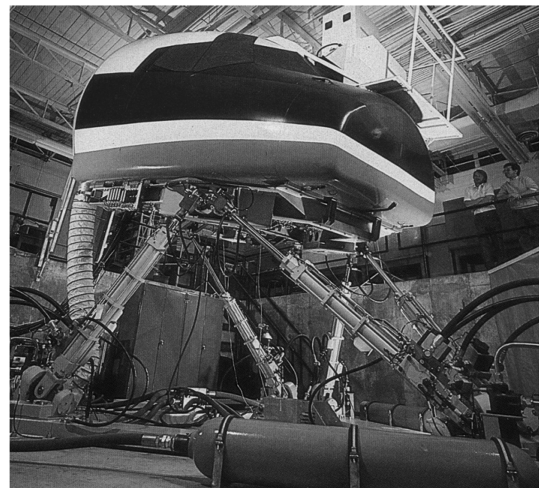


Fig. 4 UTIAS Flight Research Simulator.

orientation relative to the cab, the current value of head position relative to the cab, and the location of each eye relative to the head point to determine the inertial position and attitude of each eye. This position and attitude information is then used to render the visual scene. The lead compensates for the transport delay of the IG in response to head motions, such that the virtual world appears stationary for typical rotational head motions (i.e., close to zero delay for subject head motions) [18]. Because the goal of the experiment was to determine the phase-error threshold in a flight simulator environment, the subject's head was not restrained.

The sinusoidal pitching motion occurred about the head location of the subjects. The motion stimulated both the semicircular canals and the otoliths of the human vestibular system as the g vector tilted in the body frame of the subjects. The pitching motion was faded in over one cycle using a cubic ramp developed by Greig [12]. This ramp smoothly and consistently fades in the position, velocity, and acceleration over a cycle. After the ramp, the sinusoidal pitching motion continues for 2 cycles at 0.2 Hz (10 s) or 14 cycles at 1.0 Hz (14 s). The signal is then ramped back down to zero using the same cubic ramp.

The experiment required accurate phasing of the visual and motion signals. This was accomplished by accurately measuring the phase lag of the visual signal relative to the motion signals at the two frequencies (0.2 and 1.0 Hz). The measurements were made by comparing an actuator displacement (measured using the built-in CAE Temposonics position transducer) and the green video signal to the helmet display CRTs. A visual database with the green intensity as a linear function of pitch attitude was used to generate an electrical signal that was proportional to the pitch attitude of the displayed visual scene. The green video signal corresponds to the pitch attitude at the middle of the current screen refresh. The time delay between the zero crossings of the visual signal and the motion signal was measured using a high-speed digital sampling oscilloscope. For the interval in which the visual and motion signals were in phase, the simulator software was programmed to delay the motion signal by the measured visual lag. The delay was rounded off to an integral number of time steps of the simulation step size (1/60 s) as required by the cubic ramp algorithm. For the interval requiring motion lead, the visual signal was delayed by the appropriate number of time steps. The motion and visual synchronization measurements were done with the head tracker turned off. Because the head tracker was active during the experiment, a discussion of the head tracker effect on the synchronization of the visual and motion signals is required. The impact of the resulting synchronization errors on the results of the study will be addressed in the Results section.

A short description of the head tracker system is required to understand the effect of the head tracker on the synchronization of the motion and visual signals. The rate gyros respond to the angular velocity of the head of the subject relative to an inertial frame, whereas the Polhemus® magnetic head tracker responds to the orientation and position of the head relative to the simulator cab. A 1-deg/s dead band is applied to the rate gyro signals to eliminate noise. The time delay from the sampling of the head tracker system to the start of the corresponding refresh of the IG is 58 ms [18], and the time delay from the visual pitch command in the host computer to the start

of the corresponding refresh of the IG is 70 ms [18]. Because the measurements used to calibrate the system were taken with the head tracker off, the motion signal was in effect, delayed to coincide with the middle of the corresponding refresh of the IG from the host pitch command (a delay of 78 ms from the command). The accuracy of the motion-visual synchronization when the head tracker is active depends on the motion of the subjects' heads. Because the subjects' heads were unsupported, four different cases were analyzed to determine bounds on the synchronization error. The cases analyzed were the head stationary relative to the simulator cab, the head stationary in inertial space, a representative head movement for when the subject's neck muscles are held tight, and a representative motion for when the subject's neck muscles are loose. For the 1 Hz motion, these latter two cases correspond to the head moving with a gain of 1.2 and a phase lag of 25 deg relative to the simulator cab and a gain of 1.6 and phase lag of 30 deg relative to the simulator cab, respectively. For the 0.2 Hz case, the representative head motions are a gain of 1.1 and a phase lag of 6 deg relative to the simulator cab motion and a gain of 1.3 and a phase lag of 9 deg relative to the simulator cab. The representative head motions are based on postexperiment measurements of the head motions of a few subjects.

When the head is stationary relative to the simulator, the magnetic head tracker output is zero and the rate gyros experience the full simulator motion. The rate gyros therefore generate visual lead that was not present during the calibration. For the 1 Hz, motion gain of 1 case, an analysis of this situation shows that the visual signal (more precisely the middle of the corresponding screen refresh) will be 28.5 ms ahead of the motion signal, when in fact they were supposed to be synchronized. This is equivalent to 10.3 deg of visual lead. This result was confirmed by postexperiment measurements. This case is not achievable in practice of course, as it would require an infinitely stiff neck or the head to be restrained.

In the following analysis, it is assumed that the subject can perfectly infer the visual motion from a combination of their head motions relative to their body and the motion of the visual scene relative to their head. It is also assumed that the human can use their other motion sensors to detect the inertial motion when required. When the head is stationary relative to inertial space, there is no output from the rate gyros and the magnetic head tracker experiences the opposite motion of the simulator cab. An analysis of this situation for the 1 Hz, motion gain of 1 case, shows that the inferred visual signal will lead the motion signal by 58 ms, or 21.0 deg. This case is highly unlikely in practice, however, as the subject would need to move their head precisely out of phase with the simulator motion and postexperiment testing showed this to be almost impossible to achieve.

For the head gain of 1.2, phase lag of 25 deg (1 Hz, motion gain of 1, 5.73 deg/s pitch velocity), the inferred visual signal is calculated to be 11.0 deg ahead of the motion signal. For the head gain of the 1.6 case, phase lag of 30 deg (1 Hz, motion gain of 1, 5.73 deg/s pitch velocity), the analysis shows the visual signal is 8.6 deg ahead of the motion signal. Similarly, for the head gain of 1.1 and a phase lag of 6 deg (0.2 Hz, motion gain of 1, 5.73 deg/s pitch velocity) the analysis shows the inferred visual signal is 3.7 deg ahead of the motion signal. The analysis also predicts the inferred visual signal to

Table 3 Motion-visual synchronization errors

Frequency, Hz	Motion gain	Amplitude, deg/s	Visual lead, deg			
			Head stationary relative to cab	Head stationary in inertial space	Tight neck muscles ^a	Loose neck muscles ^b
0.2	0.5	5.73	0.8	2.4	0.7	0.5
0.2	1.0	5.73	2.5	5.1	2.4	2.1
1.0	0.5	5.73	3.1	10.8	3.7	2.3
1.0	1.0	5.73	10.3	21.0	11.0	8.6
0.2	0.5	2.29	-0.1	2.4	-0.3	-0.4
0.2	1.0	2.29	1.4	5.1	1.3	0.9
1.0	0.5	2.29	-0.9	10.8	0.15	-1.2
1.0	1.0	2.29	5.8	21.0	7.8	5.4

^aHead gain of 1.2, phase of -25 deg relative to cab for 1 Hz and head gain of 1.1 phase of -6 deg for 0.2 Hz.

^bHead gain of 1.6, phase of -30 deg relative to cab for 1 Hz and head gain of 1.3 phase of -9 deg for 0.2 Hz.

be 2.3 deg ahead of the motion signal for a head gain of 1.3 and a phase lag of 9 deg (0.2 Hz, motion gain of 1, 5.73 deg/s pitch velocity). These last four results were confirmed by postexperiment measurements. The calculated synchronization errors for all the experimental conditions are listed in Table 3. It should also be noted that the amplitude of the pitch command to the motion system was also corrected for the nonunity gain in the frequency response of the FRS [17].

The CAE helmet includes an integral headset with sound isolation around each ear. Broadband auditory noise was fed through the headset, at a volume sufficient to mask the hydraulic actuator noise.

Nine subjects, seven male and two female, between the ages of 20 and 31 years participated in the experiment. The subjects were not screened for vestibular or ocular defects. A session consisted of approximately 40 individual trials. As mentioned previously each trial consisted of two intervals. In one interval the visual and motion signals were in phase, and in the other they were out of phase by the current phase-error level determined by the Levitt procedure. At the end of each trial, the subject was required to indicate which of the two intervals contained the synchronized visual and motion cues by pushing a button. Auditory tones were used to indicate the beginning and end of the intervals and to prompt the subject for a response. In addition, an auditory tone was used to provide feedback to the subject on the correctness of their response [19]. For each trial, the synchronized motion was randomly assigned to the first or the second interval. Because the experiment was a four factor repeated measures study with two levels for each factor, each subject completed 16 sessions (2^4), for a total time of approximately 8 h. The order of presentation of the 16 sessions to a subject was random. To minimize fatigue and boredom, the subjects ran a maximum of three sessions per day with a minimum of 45 min between sessions. At the end of each session, the Kennedy simulator sickness questionnaire (SSQ) [20] was verbally administered. The experiment took approximately 5 weeks to complete.

Results

A standard repeated measures analysis of variance [21] was carried out using SYSTAT®. A treatment is considered to have a significant effect if the probability of the null hypothesis is 5% or below ($p \leq 0.05$). Effects are considered marginally significant if the probability of the null hypothesis is between 5 and 10% ($0.05 < p \leq 0.10$).

Figure 5 shows the data averaged across all conditions for each subject. The error bars indicate 1 standard deviation. As can be seen in the figure there is a large variation among subjects. Subject 3 has an average phase-error threshold of over 90 deg, which is much larger than all the other subjects' thresholds. The pooled mean across all subjects and all treatments is 57 deg with a standard deviation of 28 deg.

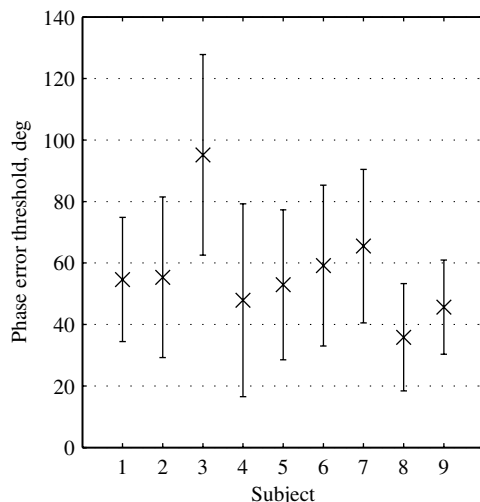


Fig. 5 Subject phase-error thresholds.

Table 4 Analysis of variance summary

Treatment	<i>p</i> value
Motion gain	0.033
Amplitude	0.0
Frequency	0.372
Visual complexity	0.509
Motion gain \times amplitude	0.419
Motion gain \times frequency	0.066
Motion gain \times visual comp.	0.264
Amplitude \times frequency	0.231
Amplitude \times visual comp.	0.835
Frequency \times visual comp.	0.260
Motion gain \times amplitude \times frequency	0.396
Motion gain \times amplitude \times visual comp.	0.987
Motion gain \times frequency \times visual comp.	0.004
Amplitude \times freq. \times visual comp.	0.391
Motion gain \times amp. \times freq. \times visual comp.	0.392

Table 4 shows a summary of the analysis of variance. As seen in the table, motion gain, amplitude (pitch velocity), and motion gain \times frequency \times visual complexity interaction all have a significant effect on the phase-error threshold and motion gain \times frequency has a marginally significant effect. The effect of amplitude is shown in Fig. 6. The error bars in this and the remaining figures depict the standard error. Smaller pitch velocities lead to larger phase-error thresholds with an average of 68 deg at 2.29 deg/s and an average of 45 deg at 5.73 deg/s. The effect of the pitch velocity can be explained by considering a signal in noise detection model. The smaller velocities lead to a smaller signal-to-noise ratio and therefore a reduction in signal information and an increase in the threshold.

Motion gain, motion gain \times frequency, and motion gain \times frequency \times visual complexity are all either significant or marginally significant. A graphical display of the three-way interaction is shown in Fig. 7. As seen in the figure the interaction appears to be due to the 1 Hz, high visual complexity, motion gain of 1 condition (averaged across both amplitudes). A simple effects test [21] was used to examine the effects of frequency and motion gain excluding the 1 Hz, high visual complexity, motion gain of 1 case. The tests found that motion gain has a significant effect ($p = 0.015$) when the frequency is 0.2 Hz, and a marginally significant effect when the visual complexity is low ($p = 0.051$). Figure 8 shows the effect of motion gain at a frequency of 0.2 Hz. The phase-error threshold decreases from 66 to 52 deg when the motion gain is increased from 0.5 to 1. Figure 9 shows the effect of motion gain at the low visual complexity. The phase-error threshold decreases from 64 to 52 deg when the gain is increased from 0.5 to 1.

The increase in the phase-error threshold as the gain is increased from 0.5 to 1 for the 1 Hz, high visual complexity case is counter to

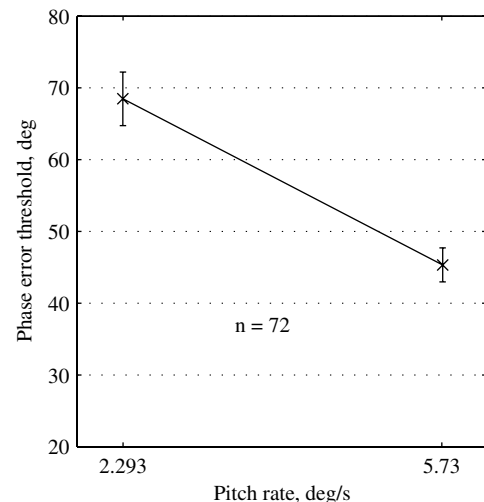


Fig. 6 Amplitude effect on phase-error threshold.

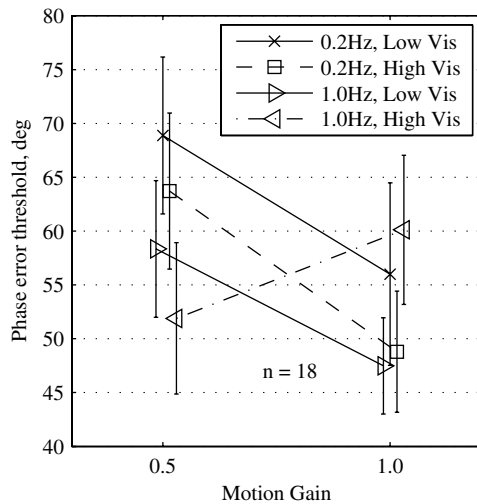


Fig. 7 Motion gain \times frequency \times visual complexity effect on phase-error threshold.

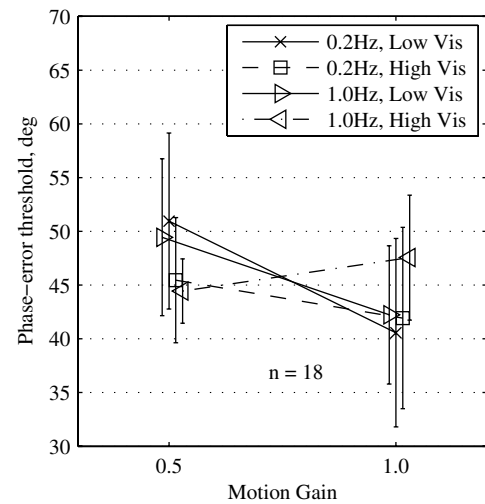


Fig. 10 Motion gain \times frequency \times visual complexity effect for pitch velocity of 5.73 deg/s.

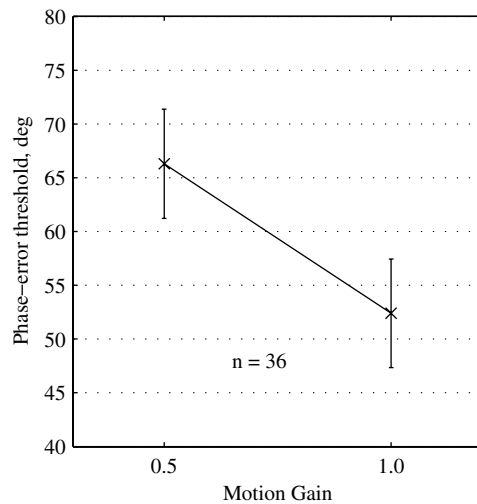


Fig. 8 Effect of motion gain at a frequency of 0.2 Hz.

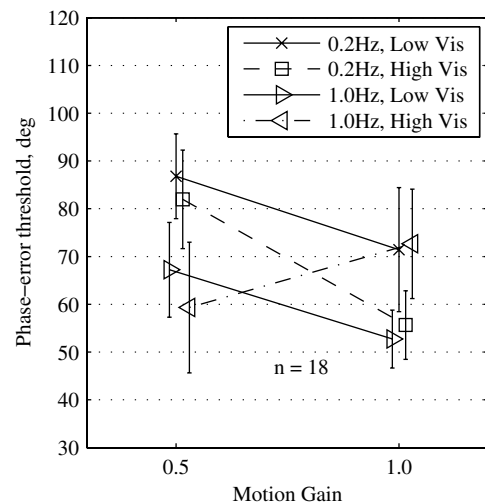


Fig. 11 Motion gain \times frequency \times visual complexity effect for pitch velocity of 2.29 deg/s.

what signal detection theory would suggest. This fact and the previous simple effects analysis suggest that the 1 Hz, high visual complexity, motion gain of 1 case may be an anomaly. The three-way interaction is therefore shown separately for the two pitch velocities in Figs. 10 and 11. The increase in phase-error threshold (at the 1 Hz,

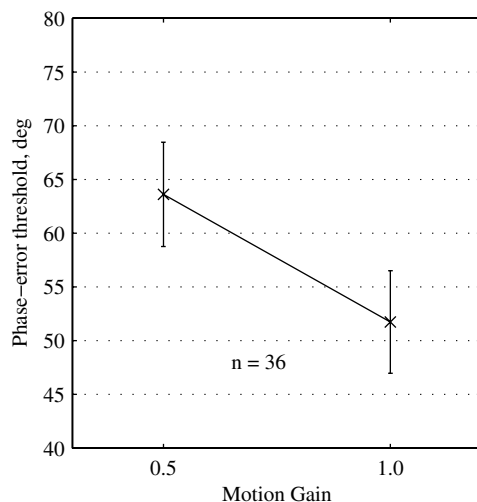


Fig. 9 Effect of motion gain at low visual complexity.

high visual complexity, motion gain of 1) occurs at both amplitudes, although more strongly at the 2.29 deg/s amplitude. As shown in Table 3, the 1 Hz, motion gain of 1 cases have the largest synchronization errors. The same synchronization errors occur at both the high and the low visual complexity but based on signal detection theory and extrapolation of the 0.2 Hz data, the expected thresholds for the high visual complexity should be lower than the low visual complexity. Therefore, one possible explanation for the increase in the phase-error threshold with the increase in gain is that the synchronization errors were large enough (relative to the phase-error threshold) that the motion and visuals did not feel in phase in either interval. Confirmation of this hypothesis requires additional experiments.

If the improbable "head stationary in inertial space" case is ignored, it can be seen from Table 3 that the synchronization errors between the visual and motion signals for these conditions (1 Hz, motion gain 1, both amplitudes) has almost a constant bias of 8 deg of visual lead. The effect of this bias is twofold. First, the bias reduces the phase lead of the motion signal relative to the visual signal for the interval where the signals were out of phase, and second, the visuals lead the motion by the bias amount for the interval when they were supposed to be in phase.

If it is assumed that the bias is substantially below the phase-error threshold (so the visual and motion signals in the "synchronized" interval are still perceived as in phase), then the results can be corrected for the synchronization errors shown in Table 3. The

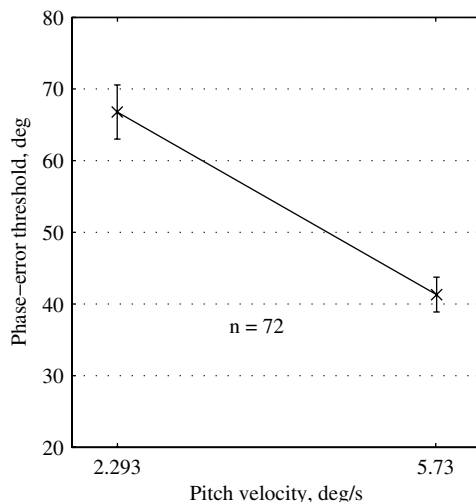
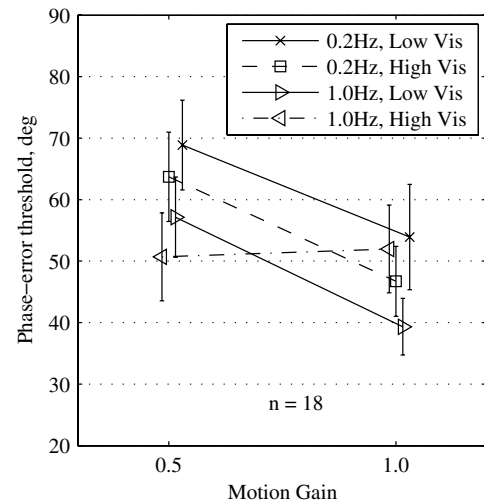
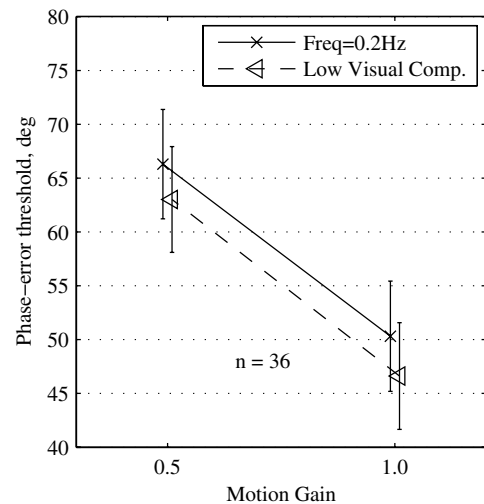
Table 5 Corrected phase-error threshold analysis of variance summary

Treatment	<i>p</i> value
Motion gain	0.004
Amplitude	0.0
Frequency	0.138
Visual complexity	0.509
Motion gain \times amplitude	0.421
Motion gain \times frequency	0.261
Motion gain \times visual comp.	0.264
Amplitude \times frequency	0.341
Amplitude \times visual comp.	0.835
Frequency \times visual comp.	0.260
Motion gain \times amplitude \times frequency	0.400
Motion gain \times amplitude \times visual comp.	0.987
Motion gain \times frequency \times visual comp.	0.004
Amplitude \times freq. \times visual comp.	0.232
Motion gain \times amp. \times freq. \times visual comp.	0.391

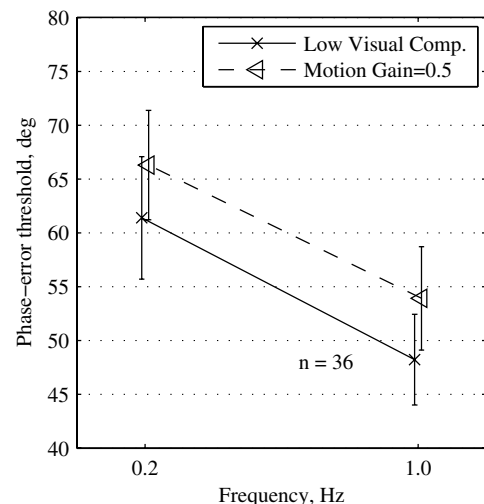
corrected phase-error thresholds can be found by subtracting the average visual lead from the measured phase-error thresholds. The average visual lead can be estimated for each experimental condition by averaging the visual leads from Table 3, for all but the head stationary in inertial space case. This correction cannot correct for cases where the bias was large enough that the in-phase interval was not perceived as such.

The correction has a very small effect on the overall results and the results averaged across subjects. Because the bias is as a function of amplitude, gain, and frequency, the analysis of variance was repeated for the corrected data, and the results of the analysis are shown in Table 5. Comparison of Table 5 with Table 4, shows the corrected results are very similar to the uncorrected results with the exception that motion gain \times frequency is no longer marginally significant. The effect of amplitude on the corrected phase-error threshold is shown in Fig. 12. Because the bias correction is larger when the motion gain is 1, the corrected phase-error threshold for this condition is substantially lower than the uncorrected phase-error threshold. The corrected phase-error threshold decreases from 67 to 41 deg when the motion gain is increased from 0.5 to 1.

The corrected three-way interaction is shown in Fig. 13. As seen in this figure, the interaction once again appears to be due to the 1 Hz, high visual complexity, and motion gain of 1 case. The corrected data, however, show an almost complete lack of interaction between the other factors (the lines which exclude the anomaly are now parallel), when compared with the uncorrected results in Fig. 7. A simple effects test was once again carried out to see if the other factors were significant when the anomaly is excluded from the analysis. Motion gain was found to be significant for the frequency of

**Fig. 12** Amplitude effect on corrected phase-error threshold.**Fig. 13** Motion gain \times frequency \times visual complexity effect on corrected phase-error threshold.**Fig. 14** Motion gain effect on corrected phase-error threshold, at frequency of 0.2 Hz and low visual complexity.

0.2 Hz ($p = 0.009$) and for the low visual complexity ($p = 0.013$). Similarly, frequency was found to be marginally significant for the motion gain of 0.5 ($p = 0.077$) and significant for the low visual complexity ($p = 0.024$). The effects of these factors on the corrected phase-error threshold are shown in Figs. 14 and 15.

**Fig. 15** Frequency effect on corrected phase-error threshold at motion gain of 0.5 and low visual complexity.

The mean of the total severity score [20] for the Kennedy SSQs was 1.91, and the largest recorded value was 14 (where the maximum is 33.66). The mean of the nausea, orientation, and oculomotor scores [20] were 1.26, 1.08, and 2.29, respectively. These scores indicate a low level of simulator sickness.

Discussion of Results

Frequency in general did not have a significant effect on the phase-error threshold except when the data were corrected for synchronization errors and only the motion gain of 0.5 or the low visual complexity conditions were considered. For these two conditions, the phase-error threshold decreased with increasing frequency. This is the opposite of what is expected if subjects behaved as time delay detectors; an increase in frequency would lead to an increase in the phase-error threshold. For example, in Fig. 15, at the low visual complexity the phase-error threshold decreases from 61 to 48 deg when the frequency increases from 0.2 to 1 Hz. The equivalent time delays are 847 ms at 0.2 Hz and 133 ms at 1 Hz. The delay difference is substantially larger than the phase difference. Similar results can be obtained for the frequency effect when the motion gain of the 0.5 case is considered. This suggests that the subjects behaved more like phase detectors rather than time delay detectors.

It is difficult to directly compare the results of this study to those of Chung and Schroeder [8] where a time delay of 85–125 ms was detectable during a helicopter lateral translation maneuver. First, the current experiment found the phase-error threshold for pitch whereas Chung and Schroeder [8] found it for a combination of roll and lateral motion. Second, the current experiment has sustained sinusoidal pitch motion which creates strongvection, which in turn may have masked the inertial pitch motion (a phenomena observed by Reid et al. [5]). Third, in the current experiment, the subjects were not actively involved in the control of a vehicle as they were in the Chung and Schroeder experiment. Involvement in a control task has been shown to increase the motion perception threshold of humans [22]. Finally, it is difficult to know which of the 16 conditions should be compared to the Chung and Schroeder experiment. Chung and Schroeder used a motion gain of 1 and employed a visual scene with a large number of vertical stripes resulting in a relatively high spatial frequency. The high visual complexity and motion gain of 1 are therefore the most appropriate levels to consider. It is more difficult to determine the appropriate frequency and amplitude to use for comparison. Figure 11 in the Chung and Schroeder [8] paper presents a time history of helicopter roll attitude. The main frequency content of the roll attitude appears to be approximately 0.2 Hz with a peak roll attitude of approximately 4 deg (resulting in a peak roll velocity of 5.6 deg/s at 0.2 Hz). The frequency content of the roll velocity is more difficult to determine because it requires differentiation of the time history data shown in the figure. Chung and Schroeder [8] did, however, use a disturbance in the study, which when filtered by the helicopter dynamics, results in a small roll velocity in the frequency band from 0.05 to 1.2 Hz. It therefore seems likely that the roll velocity had some power at both 0.2 and 1.0 Hz. At 0.2 Hz, high visual complexity, 5.73 deg/s, and a motion gain of 1 the corrected phase-error threshold was 39 deg in the current experiment. This is equivalent to 542 ms of time delay, significantly larger than the detection threshold in the Chung and Schroeder [8] experiment. The 85–125 ms for Chung experiment and 127 ms (46 deg) for the corrected phase-error threshold for the 1 Hz, motion gain of 1, 2.29 deg/s, low visual complexity case in current experiment are in reasonably good agreement. The low visual complexity case was used because the high visual complexity, high motion gain case appears to be an anomaly.

Consequences for Simulator Motion Tuning

The measured phase-error thresholds were used to analyze the MDA pitch high-pass filter response to aircraft pitch inputs. The analysis was carried out using the properties of the UTIAS FRS hardware. At low frequencies, the FRS pitch motion response can be

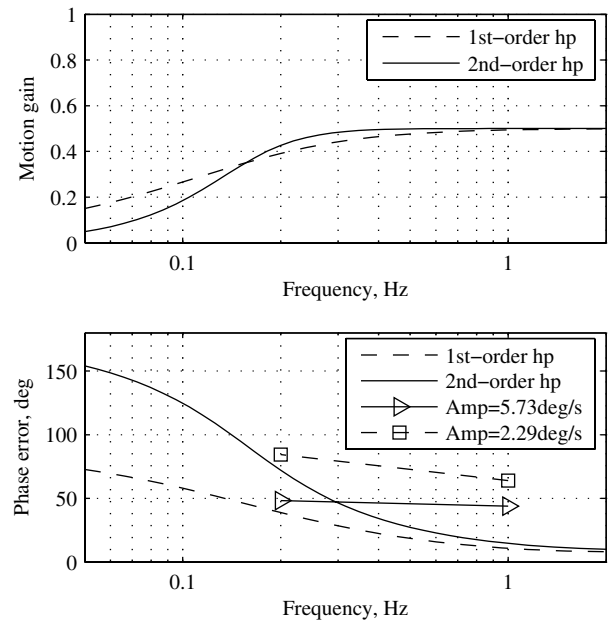


Fig. 16 Motion-visual phase error for two high-pass filters: a first-order $\omega_n = 1$ rad/s filter and a second-order $\omega_n = 1$ rad/s, $\zeta = 0.7$ filter, versus corrected phase-error thresholds.

modeled as a pure time delay of 73 ms [17]. The visual transport delay of the FRS is 78 ms. Furthermore, a motion scale factor of 0.5 was considered because this is commonly used on flight simulators. The phase error between the visual and motion signals was examined for two high-pass motion filter configurations: a first-order high-pass filter with a natural frequency (ω_n) of 1 rad/s and a second-order high-pass filter with a natural frequency of 1 rad/s, and a damping ratio (ζ) of 0.7. The total motion gain and the phase error between the motion and visual pitch for these two filters are shown in Fig. 16. Also shown on the figure are the corrected phase-error thresholds for a motion gain of 0.5 averaged over the two visual complexities and the nine subjects. The phase error for the first-order filter is below the phase-error threshold for both pitch velocities and both frequencies. For the second-order filters, the phase error intersects the threshold

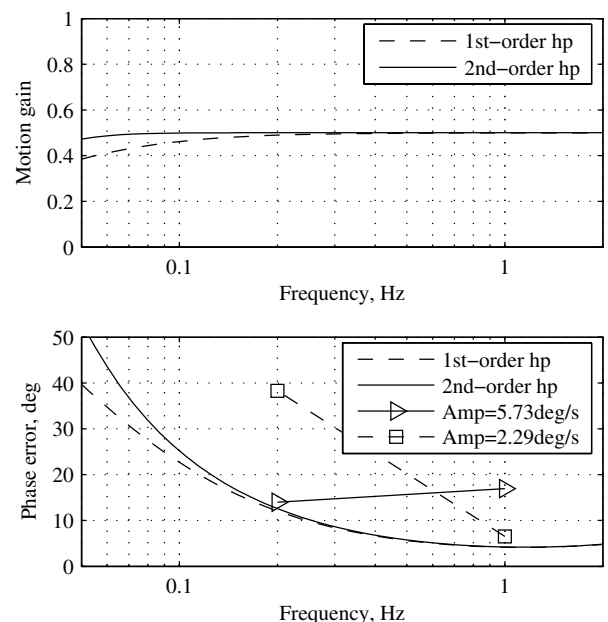


Fig. 17 Motion-visual phase error for two high-pass filters: a first-order $\omega_n = 0.19$ rad/s filter and a second-order $\omega_n = 0.13$ rad/s, $\zeta = 0.7$ filter, versus lower 95% confidence limit for corrected phase-error thresholds.

for the 5.73 deg/s pitch case at approximately 0.3 Hz. The gain is approximately 0.5 at this frequency, so for a pitch input of 5.73 deg/s, the probability of phase-error detection would be approximately 79% (assuming a linear behavior with respect to frequency). From 0.3 to 0.2 Hz the gain is rolling off very slowly and the phase is increasing quickly, so below 0.3 Hz the probability of phase-error detection is likely larger than 79% (for oscillatory inputs greater than or equal to 5.73 deg/s).

Given the large scatter in the data between subjects, it is more useful to know the largest phase error that most subjects (rather than the average subject) cannot reliably detect. Figure 17 shows the lower one-sided 95% confidence limit for the phase-error thresholds (averaged over subject and visual complexity for a motion gain of 0.5) at 0.2 and 1 Hz. These confidence intervals were based on the assumption of a Gaussian distribution. Also shown on the figure are a first-order high-pass filter with a natural frequency of 0.19 rad/s and a second-order high-pass filter with a natural frequency of 0.13 rad/s and a damping ratio of 0.7. These filter parameters were chosen such that the phase of the filters at 0.2 Hz was just below the one-sided 95% confidence interval for the phase-error threshold. These data points correspond to 5% of the subject population detecting the phase error 79% of the time. For 0.2 Hz motions, the pitch high-pass filters require very low natural frequencies to ensure most of the subjects do not detect the motion-visual phase error. If the modes of the aircraft are at 1 Hz and above, then a similar analysis shows that the first-order natural frequency and the second-order natural frequency can be raised to 0.9 and 0.63 rad/s, respectively (for 5% of the subjects to detect the motion-visual mismatch 79% of the time when the pitch velocity is less than or equal to 5.73 deg/s).

Conclusions

The human detection threshold for phase error between visual and motion cues was determined in a flight simulator environment with a helmet-mounted display for a number of different conditions. In particular, the motion-visual phase-error threshold was measured for pitch motions of 0.2 and 1 Hz, with amplitudes of 5.73 and 2.29 deg/s, motion gains of 1.0 and 0.5, and for a complex low-altitude visual scene and a simple high-altitude scene. The following conclusions can be drawn from the experiment:

- 1) The motion-visual phase-error threshold averaged across all conditions was found to be 57 deg.
- 2) The amplitude of the motion had a significant effect on the phase-error threshold with lower amplitudes leading to higher thresholds. When averaged across all other conditions, the corrected phase-error threshold was found to be 41 deg at a pitch velocity of 5.73 deg/s and 67 deg at a pitch velocity of 2.29 deg/s.
- 3) Motion gain was found to have a significant effect on the phase-error threshold when the frequency was 0.2 Hz or when the visual complexity was low. Lower gains led to higher thresholds.
- 4) Frequency was found to have a significant effect on the corrected phase-error threshold when the visual complexity was low or the motion gain was 0.5. Lower frequencies led to higher phase-error thresholds.
- 5) For the experimental conditions in this study, humans appear to operate more like motion-visual phase detectors rather than motion-visual time delay detectors.

The corrected phase-error thresholds were used to analyze high-pass pitch MDA filters. The analysis showed that break frequencies as high as 0.19 rad/s could be used for first-order high-pass filters with a low probability of detecting the motion-visual phase error. For second-order filters, however, break frequencies lower than 0.13 rad/s are required to ensure the motion-visual phase error has a low probability of detection for sustained low-frequency vehicle oscillations.

References

- [1] Young, L. R., "Visually Induced Motion in Flight Simulation," *AGARD Conference on Piloted Aircraft Environment Simulation Techniques*, CP249, AGARD, April 1978.
- [2] Frank, L. H., Casali, J. G., and Wierwille, W. W., "Effects of Visual Display and Motion System Delays on Operator Performance and Uneasiness in a Driving Simulator," *Human Factors*, Vol. 30, No. 2, 1988, pp. 201–217.
- [3] Young, L. R., Dichgans, J., Murphy, R., and Brandt, Th., "Interaction of Optokinetic and Vestibular Stimuli in Motion Perception," *Acta Otolaryng*, Vol. 76, No. 1, 1973, pp. 24–31.
- [4] Hosman, R. J. A. W., and van der Vaart, J. C., "Visual-Vestibular Interaction in Pilot's Perception of Aircraft or Simulator Motion," *AIAA Flight Simulation Technologies Conference*, AIAA Paper 88-4622-CP, 1988, pp. 271–280.
- [5] Reid, L. D., Grant, P. R., and Greig, G. L., "The Interaction Between Visually Induced Motion and Physical Motion in a Flight Simulator," *Society for Computer Simulation Conference Proceedings*, The Society for Computer Simulation, San Diego, CA, 1987, pp. 724–729.
- [6] Shirachi, D. K., and Shirley, R. S., "Visual/Motion Cue Mismatch in a Coordinated Roll Maneuver," NASA CR 166259, 1981.
- [7] Miller, G. K., and Riley, D. R., "The Effect of Visual-Motion Time Delays on Pilot Performance in a Simulated Pursuit Tracking Task," NASA TN D-8364, 1977.
- [8] Chung, W. W., and Schroeder, J. A., "Visual and Roll-Lateral Motion Cueing Synchronization Requirements for Motion-Based Flight Simulations," *American Helicopter Society 53rd Annual Forum*, American Helicopter Society International, Alexandria, VA, 1997.
- [9] Waszak, M. R., and Schmidt, D. K., "Flight Dynamics of Aeroelastic Vehicles," *Journal of Aircraft*, Vol. 25, No. 6, June 1988, pp. 563–571.
- [10] Reid, L. D., and Nahon, M., "Flight Simulator Motion-Base Drive Algorithms: Part 2—Selecting the System Parameters," UTIAS Rept. 307, 1986.
- [11] Farrell, R. J., and Booth, J. M., "Design Handbook for Imagery Interpretation and Equipment," Boeing Aerospace Company, AD/A-025 453, U.S. Department of Commerce, National Technical Information Service, Dec. 1975.
- [12] Greig, G. L., "Masking of Motion Cues by Random Motion: Comparison of Human Performance with a Signal Detection Model," UTIAS Rept. 313, 1988.
- [13] Forsstrom, K. S., Doty, J., and Cardullo, F. M., "Using Human Motion Perception Models to Optimize Flight Simulator Motion Algorithms," *Proceedings of the AIAA Flight Simulation Technologies Conference*, AIAA, New York, 1985, pp. 46–51; also AIAA Paper 85-1743.
- [14] Levitt, H., "Transformed Up-Down Methods in Psychoacoustics," *Journal of the Acoustical Society of America*, Vol. 49, No. 2, 1971, pp. 467–477.
- [15] Dember, W. N., and Warm, J. S., *Psychology of Perception*, 2nd ed., Holt, Reinhart, and Winston, New York, 1979, Chap. 2.
- [16] Leek, M. R., "Adaptive Procedures in Psychophysical Research," *Perception and Psychophysics*, Vol. 63, No. 8, Nov. 2001, pp. 1279–1292.
- [17] Grant, P. R., "Motion Characteristics of the UTIAS Flight Research Simulator Motion-Base," UTIAS TN 261, 1986.
- [18] Reid, L. D., Sattler, D. E., Graf, W. O., Dufort, P. A., and Zielinski, A. W., "Cockpit Technology Simulation Development Study for Enhanced/Synthetic Vision System," UTIAS Rept. 355, Nov. 1998.
- [19] Lukaszewski, J. S., and Elliott, D. N., "Auditory Threshold as a Function of Forced-Choice Technique, Feedback, and Motivation," *Journal of the Acoustical Society of America*, Vol. 34, No. 2, Feb. 1962, pp. 223–228.
- [20] Kennedy, R. S., Lane, N. E., Berbaum, K. S., and Lilienthal, M. G., "Simulator Sickness Questionnaire: An Enhanced Method for Quantifying Simulator Sickness," *International Journal of Aviation Psychology*, Vol. 3, No. 3, 1993, pp. 203–220.
- [21] Neter, J., Wasserman, W., and Kutner, M. H., *Applied Linear Statistical Models*, 3rd ed., Irwin, Homewood, 1990.
- [22] Samji, A., and Reid, L. D., "The Detection of Low Amplitude Yawing Motion Transients in a Flight Simulator," *IEEE Transactions of Systems, Man, and Cybernetics*, Vol. 22, No. 2, March/April 1992, pp. 300–306.